Quantum Information Processing (2020) 19:362
https://doi.org/10.1007/s11128-020-02868-2

A novel coherence-based quantum steganalysis protocol

Zhiguo Qu[1,2,3] · **Yiming Huang**[4] · **Min Zheng**[5]

Received: 13 May 2020 / Accepted: 14 September 2020

Abstract
The quantum steganalysis faces more challenges than classical steganalysis owing to the support of quantum mechanical principles such as Heisenberg uncertainty principle and non-cloning theorem. In this paper, a novel quantum steganalysis protocol based on pure state is proposed, which adheres to the fundamental fact that classical steganography tends to change the probability distribution of the carrier, and the physical properties that the unknown quantum state discrimination process is sensitive to the distribution in quantum state discrimination. After utilizing accurate calculation on the geometric coherence and 1/2-affinity coherence to obtain the probability that the transmitted quantum states can be correctly discriminated, effective detection on covert communication can be achieved by comparing the detected distribution with theoretical distribution. Meanwhile, steganographic detection rate and false alarm rate are introduced as two significant performance evaluation parameters of quantum steganalysis. In this paper, the quantum steganalysis and performance evaluation targeting the BB84-based quantum steganography proposed by Martin are given in detail. The geometric coherence and 1/2-affinity coherence change substantially when the steganographic embedding rate is above 0.2, and a high steganographic detection rate and a low false alarm rate can be obtained according to the proposed protocol. Besides, the impact on QKD efficiency can be controlled by adjusting the detection rate or adopting sampling detection strategy. It proves that the proposed protocol has a satisfactory quantum steganalysis performance.

Keywords Quantum steganalysis · Quantum coherence · Quantum state discrimination · Quantum covert communication

1 Introduction

As one of the significant research fields of information security, classical steganography aims at protecting information transmission. It can realize covert communication by establishing a hidden channel in the open channel without causing suspicion.As an extension of classical steganography in the quantum field, quantum steganography

Extended author information available on the last page of the article

Published online: 26 September 2020

has developed for decades by integrating the fundamental idea of classical steganography into quantum secure communications. Compared with classical steganography, quantum steganography has more natural advantages and broader prospects in terms of imperceptibility, capacity and security due to various particular physical properties of quantum, such as Heisenberg uncertainty principle and quantum non-cloning principle, etc.

Quantum steganography has developed rapidly in the last decade. In general, it can be divided into the following three categories: quantum data hiding, quantum covert communication and quantum multimedia steganography. Firstly, quantum data hiding (QDH) mainly employs quantum mechanical properties to hide secret messages. Terhal et al. [1] proposed the first QDH protocol based on the property that $\left|\Phi^{-}\right\rangle$ is a spin singlet unique to four Bell states. Guo and Guo [2] analyzed the implementation of QDH with Bell states using an optical frequency converter and simplified the coding process. Eggeling and Werner [3] realized data hiding in multi-particle non-entangled quantum states. Matthews et al. [4] investigated how to distinguish quantum states with limited measurements, which is of great use to QDH. Various quantum steganography schemes [5–9] were proposed recently utilizing particular quantum states, such as GHZ states, Brown states. Quantum covert communication (QCC) is a vital branch of quantum steganography. It realizes covert communication based on quantum secure communication. Gea-Banacloche [10] implemented the covert transmission based on quantum error-correcting codes (QECC). Martin [11] put forward novel steganography based on BB84 protocol [12], which could hide a secret bit in the eavesdropping detection particles. The protocol is widely used because it is easy to implement physically by only using single-particle state. Liao et al. [13] designed a steganography protocol based on quantum secret sharing (QSS). Several quantum steganography schemes [14–16] were proposed based on the quantum secure direct communication protocol (QSDC). Mihara [17,18] and Qu et al. [19] designed quantum steganography based on entanglement and QECC. The third category is quantum multimedia steganography (QMS), which is of high steganographic capacity. It realizes covert communication by embedding secret messages into quantum multimedia, such as quantum text, quantum image, quantum audio [20], quantum video. It is a promising branch and has been developing rapidly in recent years. Mogo [21,22] expanded the application of classical information hiding to the quantum field by using three-dimensional qubits to represent image pixel values. Jiang and Wang [23] proposed a quantum image steganography protocol based on Moire pattern. Enhanced quantum representation (NEQR) and least significant bit (LSB) are widely used in QMS [20,24–29].

On the contrary, steganalysis targets to prevent covert communication by detecting the existence of hidden channel in open channel. It is easy to know that the relationship between steganalysis and steganography is similar to that of spear and shield. Meanwhile, steganography and steganalysis also will complement each other. In other words, steganalysis plays a crucial role in promoting the development of steganography, while the progress of steganography reversely provides new challenges and opportunities for the development of steganalysis.

The flourishing of quantum steganography in the last decade further increases the urgency and importance of the research on quantum steganalysis for the effective detection of covert communication. However, there exist more challenges to over-

come for quantum steganalysis due to quantum properties, such as the Heisenberg uncertainty principle and quantum non-cloning principle. The relevant development is still in the embryonic stage. There are only a few quantum steganalysis schemes targeting QMS, which attempt to detect secret messages in the carrier utilizing feature extraction techniques and machine learning algorithms. Luo et al. [30] came up with a quantum steganalysis scheme for LSB-based quantum image steganography and designed a series of simple quantum circuits to accomplish the steganalysis procedure. Chaharlang et al. [31,32] proposed two quantum audio steganography protocols based on the least significant fractional qubit and performed corresponding quantum steganalysis utilizing quantum K-nearest neighbor algorithm and quantum circuits network.

Nevertheless, the research on quantum steganalysis of other two types of quantum steganography (QDH and QCC) is still close to blank at present. In particular, QCC protocols based on quantum secure communication protocols have a promising application prospect, since quantum secure communication protocols are the basis of future quantum communication networks. Therefore, it is of great practical significance and theoretical value to develop quantum steganalysis targeting QCC. Under these circumstances, a novel coherence-based quantum steganalysis protocol based on pure state is presented in this paper, which adheres to the essential fact that classical steganography tends to change the probability distribution of the carrier and the physical characteristics that the unknown quantum state discrimination process is sensitive to the distribution in quantum state discrimination. In the new protocol, by accurate calculation on the geometric coherence and 1/2-affinity coherence to obtain the probability that the transmitted quantum states can be correctly discriminated, effective detection on covert communication can be achieved by analyzing the difference between the detected distribution and the theoretical distribution.

The remainder of this paper is organized as follows. A brief introduction to basic definitions and related formulas used in this paper is given in Sect. 2. Section 3 presents the overall flow chart and specific execution steps of the new protocol. In Sect. 4, the quantum steganography protocol [11] proposed by Martin is utilized to illustrate the process of quantum steganalysis concretely. The performance analysis of the proposed quantum steganalysis protocol is given in Sect. 5. This paper is ended up with discussions and conclusions in Sect. 6.

2 Preliminaries

2.1 Fidelity and affinity

Distance in quantum state space is fundamental for quantifying correlation. Inner product $|\langle\psi|\varphi\rangle|$ can be used describe the distance between two pure quantum states $|\psi\rangle$ and $|\varphi\rangle$. For general quantum states ρ and σ, their fidelity and affinity can also be used as the measurements on their distance [33,34].

Fidelity is defined by Eq. (1).

$$F(\rho, \sigma) = tr\left(\sqrt{\rho^{1/2}\sigma\rho^{1/2}}\right) \tag{1}$$

Affinity is defined by Eq. (2).

$$A(\rho, \sigma) = tr\left(\sqrt{\rho}\sqrt{\sigma}\right) \tag{2}$$

As a generalization of affinity, α-affinity is defined by Eq. (3).

$$A^{(\alpha)}(\rho, \sigma) = tr\left(\rho^{\alpha}\sigma^{1-\alpha}\right) \tag{3}$$

Here, $\alpha \in (0, 1)$.

Fidelity and affinity are the generalizations of classical distance, in a certain sense. They both represent the degree of proximity between two arbitrary quantum states in the Hilbert space.

2.2 Coherent and incoherent quantum states

Coherence is one of the fundamental characteristics of a quantum system, which reflects the wave properties. As a precious quantum resource, coherence has been widely studied in many fields.

Given an orthonormal basis $\{|i\rangle, i = 1, 2, \ldots, d\}$ on a d-dimensional Hilbert space $\mathcal{H}$, the incoherent state can be represented by a density matrix with diagonal form. The collection of incoherent states is given as

$$\mathcal{I} = \left\{\sigma | \sigma = \sum_{i=1}^{d} \lambda_i |i\rangle \langle i|, \lambda_i > 0, \sum_i \lambda_i = 1\right\} \tag{4}$$

On the contrary, the quantum state that cannot be denoted as such diagonal matrix form is defined as the coherent state.

2.3 Several kinds of coherence

Baumgratz et al. [35] proposed a rigorous framework of resource theory to study coherence based on the idea of quantifying entanglement, and they listed four properties (faithful, monotonicity, strong monotonicity, and convexity) that the coherence measures should satisfy. Several kinds of coherence have been proposed on this framework.

Geometric coherence [36] is defined by Eq. (5).

$$C_g(\rho) = 1 - \max_{\sigma \in \mathcal{I}} F^2(\rho, \sigma) \tag{5}$$

Here, $\mathcal{I}$ is the set of incoherence states.

Affinity coherence [37] is defined by Eq. (6).

$$\widetilde{C}_a(\rho) = 1 - \max_{\sigma \in \mathcal{I}} A(\rho, \sigma) \tag{6}$$

Here, $\mathcal{I}$ is the set of incoherence states.

α-affinity coherence is defined by Eq. (7).

$$C_a^{(\alpha)}(\rho) = 1 - \max_{\sigma \in \mathcal{I}} \left[tr\left(\rho^{\alpha} \sigma^{1-\alpha}\right)\right]^{1/\alpha} \tag{7}$$

Here, $\mathcal{I}$ is the set of incoherence states.

The authors in [38] deduced the upper and lower bounds of geometric coherence according to the super-fidelity and sub-fidelity, denoted by Eq. (8).

$$\widetilde{C}_a(\rho) < C_g(\rho) < \min\{l_1, l_2\} \tag{8}$$

Here, $\widetilde{C}_a(\rho) = 1 - \sqrt{\sum_i \langle i| \sqrt{\rho} |i\rangle}$, $l_1 = 1 - \max_i \{\rho_{ii}\}$, $l_2 = 1 - \sum_i b_{ii}^2$ and $\sqrt{\rho} = \sum_{i,j} b_{ij} |i\rangle \langle j|$.

By polar decomposition, it can be driven that $\sqrt{\rho^{1/2} \sigma \rho^{1/2}} = \sqrt{\rho}\sqrt{\sigma} U$; therefore, it can also be easily proved by definition that 1/2-affinity coherence is an upper bound for geometric coherence.

$$C_g(\rho) \leq C_a^{1/2}(\rho) \tag{9}$$

For an arbitrary incoherence state σ that can be described as $\sigma = \sum_{i=1}^{d} \lambda_i |i\rangle \langle i|$, the analytic expression of α-affinity coherence of ρ [37] is given by Eq. (10).

$$C_a^{(\alpha)}(\rho) = 1 - \sum_i \langle i| \rho^{\alpha} |i\rangle^{1/\alpha} \tag{10}$$

Geometric coherence and α-affinity coherence satisfy the properties of coherence measures proposed by Baumgratz. The affinity coherence does not meet the strong monotonicity, and it is a kind of convex weak coherence.

2.4 Quantum state discrimination

2.4.1 Unknown quantum state discrimination

Let us assume that the public channel considered by Charlie is $\{\rho_i, \eta_i\}_{i=1}^{d}$. In other words, Charlie believes that Alice takes the probability of η_i to send the quantum state ρ_i. Charlie performs a measurement operation to discriminate the quantum states that Alice sends. In general, Charlie can choose to use positive operator-valued measure (POVM), and POVM is a set of semi-positive definite operators M_i that satisfy the completeness.

The probability that Charlie receives ρ_j and determines it is ρ_i and can be denoted as $p(i|j) = tr\left(M_i \rho_j\right)$. Hence, the maximum probability that Charlie can correctly discriminate all quantum states is given by Eq. (11).

$$P_S^{opt}\left(\{\rho_i, \eta_i\}_{i=1}^d\right) = \max_{M_i} \sum_i \eta_i tr\left(M_i \rho_i\right) \tag{11}$$

Here, the maximum value can be achieved by traversing all the possible POVM operators.

2.4.2 Discriminate states using least square measure

Belavkin [39], Holevo [40], and Eldar and Forney [41] proposed the least square measurement (LSM) from the perspective of multivariate quantum statistical hypothesis testing. The construction of LSM is simple and can be obtained directly according to the quantum states to be measured. Moreover, the probability of successfully discriminating states by LSM is nearly optimal when the quantum states to be distinguished are nearly orthogonal [40,42].

For the pure states $\{|\varphi_i\rangle, \eta_i\}_{i=1}^d$ with prior probability η_i, the LSM is given as follows.

$$\left|f_i^{\text{lsm}}\right\rangle = \sqrt{\eta_i}\left(\sum_i \eta_i\right)^{-1/2} |\varphi_i\rangle, \quad i = 1, 2, \ldots, d \tag{12}$$

For the mixed states $\{\rho_i, \eta_i\}_{i=1}^d$ with prior probability, the LSM is given as

$$M_i^{\text{lsm}} = \eta_i \rho_{\text{out}}^{-1/2} \rho_i \rho_{\text{out}}^{-1/2}, \quad i = 1, 2, \ldots, d \tag{13}$$

Here, $\rho_{\text{out}} = \sum_i \eta_i \rho_i$.

3 The proposed coherence-based quantum steganalysis algorithm

Let us suppose that there exists a monitor Charlie when Alice and Bob are communicating with each other through public quantum channel. Charlie's responsibility is to detect the existence of hidden channel and prevent the transmission of secret messages. In this case, the communication process between Alice and Bob is shown in Fig. 1.

If Charlie suspects that secret messages are embedded in open quantum channel, he can intercept and use appropriate measurement operators to measure the states transferred between Alice and Bob with probabilities. By discriminating the transmitted quantum states, he is likely to detect the existence of covert communication. Therefore, the probability that Charlie can correctly discriminate the transmitted quantum states is crucial for the quantum steganalysis. The brief flowchart of detecting covert communication is shown in Fig. 2.

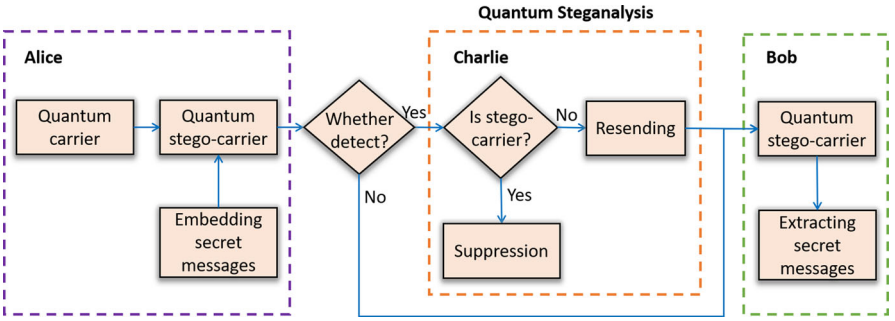

Fig. 1 The architecture of quantum steganography–steganalysis system

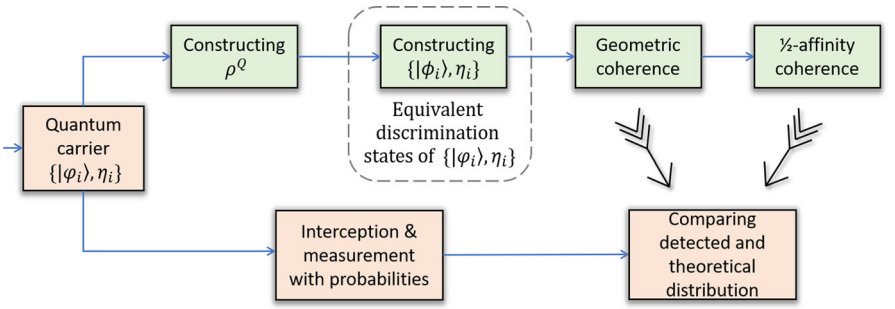

Fig. 2 The flowchart of the coherence-based quantum steganalysis

Firstly, according to the distribution $\{\rho_i, \eta_i\}_{i=1}^d$ that Charlie holds, a mathematical matrix ρ^Q can be constructed when public quantum channel is transmitting pure quantum states, i.e., the transmitted quantum states can be expressed as $\rho_i = |\varphi_i\rangle \langle\varphi_i|$. And then, a collection of states that could be discriminated with equal probability is constructed based on ρ^Q, which are named as equivalent discrimination states and denoted as $\{|\phi_i\rangle, \eta_i\}_{i=1}^d$. Accordingly, the discrimination issue of $\{|\varphi_i\rangle, \eta_i\}_{i=1}^d$ is transformed into the discrimination of $\{|\phi_i\rangle, \eta_i\}_{i=1}^d$. The geometric coherence and 1/2-affinity coherence of ρ^Q are closely related to the probability of discriminating $\{|\phi_i\rangle, \eta_i\}_{i=1}^d$. Therefore, geometric coherence and 1/2-affinity coherence of ρ^Q act as essential indexes in quantum steganalysis. Since that there exists no analytic expression of geometric coherence, and geometric coherence is also hard to calculate in some cases, 1/2-affinity coherence is calculated instead of geometric coherence. Finally, Charlie measures the quantum states in public channel with a certain probability and realizes effective detection on covert communication by analyzing the difference between the detected distribution with theoretical distribution.

According to Fig. 2, the specific steps of the coherence-based quantum steganalysis protocol are given as follows.

Step 1: Constructing the density matrix ρ^Q

A mathematical density matrix $\rho^{Q} = \sum_{i,j} \sqrt{\eta_i \eta_j} \langle \varphi_i | \varphi_j \rangle |i\rangle \langle j|$ can be constructed based on the distribution of quantum channels $\{|\varphi_i\rangle, \eta_i\}_{i=1}^{d}$, which is denoted as

$$\rho^{Q} = \begin{pmatrix} \eta_1 & \sqrt{\eta_1 \eta_2} \langle \varphi_1 | \varphi_2 \rangle & \cdots & \sqrt{\eta_1 \eta_d} \langle \varphi_1 | \varphi_d \rangle \\ \sqrt{\eta_2 \eta_1} \langle \varphi_2 | \varphi_1 \rangle & \eta_2 & \cdots & \sqrt{\eta_2 \eta_d} \langle \varphi_2 | \varphi_d \rangle \\ \vdots & \vdots & \ddots & \vdots \\ \sqrt{\eta_d \eta_1} \langle \varphi_d | \varphi_1 \rangle & \sqrt{\eta_d \eta_2} \langle \varphi_d | \varphi_2 \rangle & \cdots & \eta_d \end{pmatrix} \tag{14}$$

Step 2: Constructing the equivalent discrimination states $\{|\phi_i\rangle, \eta_i\}_{i=1}^{d}$

According to the ρ^{Q} constructed in the previous step, a new ensemble $\{|\phi_i\rangle, \eta_i\}_{i=1}^{d}$ can be constructed, which are the equivalent discrimination states of $\{|\varphi_i\rangle, \eta_i\}_{i=1}^{d}$. They are denoted as follows.

$$|\phi_i\rangle = \frac{\sqrt{\rho^{Q}}}{\sqrt{\eta_i}} |i\rangle \tag{15}$$

It is easy to deduce that $\langle \varphi_i | \varphi_j \rangle = \langle \phi_i | \phi_j \rangle$.

The discrimination issue of $\{|\varphi_i\rangle, \eta_i\}_{i=1}^{d}$ is equivalent to the discrimination of $\{|\phi_i\rangle, \eta_i\}_{i=1}^{d}$ according to the conclusion [38] that $P_S^{\text{optv.N}}\left(\{|\varphi_i\rangle, \eta_i\}_{i=1}^{d}\right) = P_S^{\text{optv.N}}\left(\{|\phi_i\rangle, \eta_i\}_{i=1}^{d}\right)$ and $P_S^{\text{lsm}}\left(\{|\varphi_i\rangle, \eta_i\}_{i=1}^{d}\right) = P_S^{\text{lsm}}\left(\{|\phi_i\rangle, \eta_i\}_{i=1}^{d}\right)$. Therefore, $\{|\varphi_i\rangle, \eta_i\}_{i=1}^{d}$ and $\{|\phi_i\rangle, \eta_i\}_{i=1}^{d}$ are called as equivalent discrimination states.

Step 3: Calculating the geometric coherence of ρ^{Q}

The geometric coherence of ρ^{Q} is equal to the error probability of discriminating $\{|\varphi_i\rangle, \eta_i\}_{i=1}^{d}$ under the optimal von Neumann measurement.

$$P_E^{\text{optv.N}}\left(\{|\varphi_i\rangle, \eta_i\}_{i=1}^{d}\right) = C_g\left(\rho^{Q}\right) \tag{16}$$

Equation (16) is reasonable due to the conclusion that geometric coherence of ρ^{Q} is equal to the error probability of discriminating $\{|\phi_i\rangle, \eta_i\}_{i=1}^{d}\left(|\phi_i\rangle = \frac{\sqrt{\rho^{Q}}}{\sqrt{\eta_i}} |i\rangle\right)$ by the optimal von Neumann measurement [43].

$$C_g\left(\rho^{Q}\right) = P_E^{\text{optv.N}}\left(\{|\phi_i\rangle, \eta_i\}_{i=1}^{d}\right) \geq P_E^{opt}\left(\{|\phi_i\rangle, \eta_i\}_{i=1}^{d}\right) \tag{17}$$

The optimal value can be obtained for von Neumann measurement when $\{|\phi_i\rangle\}_{i=1}^{d}$ are linearly independent. Hence the geometric coherence of ρ^{Q} is exactly equal to the minimum error probability on the premise that $\{|\phi_i\rangle\}_{i=1}^{d}$ are linearly independent. Equation (16) is reasonable because of Eq. (17) and the fact that $\{|\phi_i\rangle, \eta_i\}_{i=1}^{d}$ and $\{|\varphi_i\rangle, \eta_i\}_{i=1}^{d}$ are equivalent discrimination states.

Step 4: Calculating the 1/2-affinity coherence of ρ^{Q}

1/2-affinity coherence is a suboptimal choice since geometric coherence has no analytic formula yet. A similar conclusion can be derived that the 1/2-affinity coherence

of ρ^Q equals to the error probability of discriminating $\{|\varphi_i\rangle, \eta_i\}_{i=1}^d$ with LSM.

$$C_a^{1/2}\left(\rho^Q\right) = P_E^{\text{lsm}}\left(\{|\varphi_i\rangle, \eta_i\}_{i=1}^d\right) \tag{18}$$

The proof of Eq. (18) is as follows. Since $\rho^Q = \sum_i \eta_i |\phi_i\rangle\langle\phi_i|$, the corresponding least square measurement is $M_i^{\text{lsm}} = \eta_i\left(\rho^Q\right)^{-1/2}|\phi_i\rangle\langle\phi_i|\left(\rho^Q\right)^{-1/2} = |i\rangle\langle i|$. According to Eq. (11), the probability of successfully discriminating $\{|\phi_i\rangle, \eta_i\}_{i=1}^d$ with LSM is given by Eq. (19).

$$\begin{aligned} P_S^{\text{lsm}}\left(\{|\phi_i\rangle, \eta_i\}_{i=1}^d\right) &= \sum_i \eta_i tr\left(M_i^{\text{lsm}}|\phi_i\rangle\langle\phi_i|\right) \\ &= \sum_i \eta_i \langle\phi_i|i\rangle\langle i|\phi_i\rangle \\ &= \sum_i \langle i|\sqrt{\rho^Q}|i\rangle^2 \end{aligned} \tag{19}$$

$$P_E^{\text{lsm}}\left(\{|\phi_i\rangle, \eta_i\}_{i=1}^d\right) = 1 - \sum_i \langle i|\sqrt{\rho^Q}|i\rangle^2 \tag{20}$$

Equation (20) happens to be the same as the expression of α-affinity coherence in Eq. (10) when $\alpha = 1/2$. In order to maintain a unified mathematical form and physical interpretation of geometric coherence, Eq. (20) can be rewritten as Eq. (21).

$$C_a^{1/2}\left(\rho^Q\right) = P_E^{\text{lsm}}\left(\{|\phi_i\rangle, \eta_i\}_{i=1}^d\right) \tag{21}$$

Equation (18) is reasonable because of Eq. (21) and the result that $\{|\phi_i\rangle, \eta_i\}_{i=1}^d$ and $\{|\varphi_i\rangle, \eta_i\}_{i=1}^d$ are equivalent discrimination states. Besides, 1/2-affinity is an upper bound for geometric coherence, according to Eq. (9), and 1/2-affinity can be used when geometric coherence is too complex to be calculated.

Step 5: Detecting covert communication

Charlie detects public quantum channel and measures the qubits with a certain probability k. Detection rate k is closely related to communication efficiency. The existence of covert communication can be detected by utilizing relative entropy to measure the difference between the detected distribution $p(x)$ and the theoretical distribution $q(x)$. During the quantum steganalysis procedure, a threshold ξ needs to be set. If the difference exceeds the threshold ξ,

$$\text{KL}\left(p(x)||q(x)\right) = \sum_x p(x)\log\frac{p(x)}{q(x)} \geq \xi \tag{22}$$

Charlie believes in the existence of covert communication and suppresses the transmission. Otherwise, Charlie resends the measured particles to Bob directly.

In order to illustrate the steps of the new protocol more clearly, the following content makes a detailed steganalysis to the quantum steganography protocol [11] based on BB84 [12] proposed by Martin.

4 Steganalysis of BB84-based quantum steganography protocol

Martin proposed a quantum steganography protocol based on the QKD-BB84 protocol. Let the qubits transmitted are $|0\rangle, |1\rangle, |+\rangle$ and $|-\rangle$ with the prior probability η_i $(i = 1, 2, 3, 4)$. ρ^Q can be calculated according to Eq. (14).

$$\rho^Q = \begin{pmatrix} \eta_1 & 0 & \sqrt{\eta_1\eta_3/2} & \sqrt{\eta_1\eta_4/2} \\ 0 & \eta_2 & \sqrt{\eta_2\eta_3/2} & -\sqrt{\eta_2\eta_4/2} \\ \sqrt{\eta_3\eta_1/2} & \sqrt{\eta_3\eta_2/2} & \eta_3 & 0 \\ \sqrt{\eta_4\eta_1/2} & -\sqrt{\eta_4\eta_2/2} & 0 & \eta_4 \end{pmatrix}$$

When the public channel has no secret message for transmission, i.e., $\eta_1 = \eta_2 = \eta_3 = \eta_4 = \frac{1}{4}$. According to Eq. (15), the equivalent discrimination states are denoted as follows:

$$|\phi_1\rangle = \begin{pmatrix} \frac{1}{\sqrt{2}} \\ 0 \\ \frac{1}{2} \\ \frac{1}{2} \end{pmatrix} |\phi_2\rangle = \begin{pmatrix} 0 \\ \frac{1}{\sqrt{2}} \\ \frac{1}{2} \\ -\frac{1}{2} \end{pmatrix} |\phi_3\rangle = \begin{pmatrix} \frac{1}{2} \\ \frac{1}{2} \\ \frac{1}{\sqrt{2}} \\ 0 \end{pmatrix} |\phi_4\rangle = \begin{pmatrix} \frac{1}{2} \\ -\frac{1}{2} \\ 0 \\ \frac{1}{\sqrt{2}} \end{pmatrix}$$

$C_a^{1/2}\left(\rho^Q\right) = 0.5$ can be calculated by Eq. (10), and $C_g\left(\rho^Q\right) = 0.5$ can also be figured out by using numerical methods according to the definition. Based on these two kinds of coherence, the error rate of discriminating transmitted quantum states by Charlie is nearly 0.5. It shows that geometric coherence and 1/2-affinity coherence have little difference when there does not exist covert communication in this quantum steganography protocol.

In the quantum steganography protocol, the embedding rate (E) is defined as the ratio between the bit number of secret messages and the total number of carrier bits, denoted by Eq. (23).

$$\text{Embedding rate } (E) = \frac{\text{The bit number of secret message}}{\text{The total number of carrier bits}} \tag{23}$$

The number of carrier bits is $4n$ in the BB84-based quantum steganography protocol, but the actual length of the distributed key is n. Therefore, n is used for the number of carrier bits when calculating E in this paper. The steganography capacity of the original protocol is only one bit. The protocol needs to be repeated multiple times if secret messages to be transmitted are more than one bit.

The quantum steganography protocol can hide classical message '0' or '1.' It might as well assume the embedded secret messages are '0.' Therefore, the quantum channel is $\{|\varphi_i\rangle, \eta_i\}_{i=1}^4$, here $|\varphi_i\rangle = \{|0\rangle, |1\rangle, |+\rangle, |-\rangle\}$ and $\eta_i = \left\{\frac{n-nE}{4n} + \frac{nE}{2n}, \frac{n-nE}{4n},\right.$

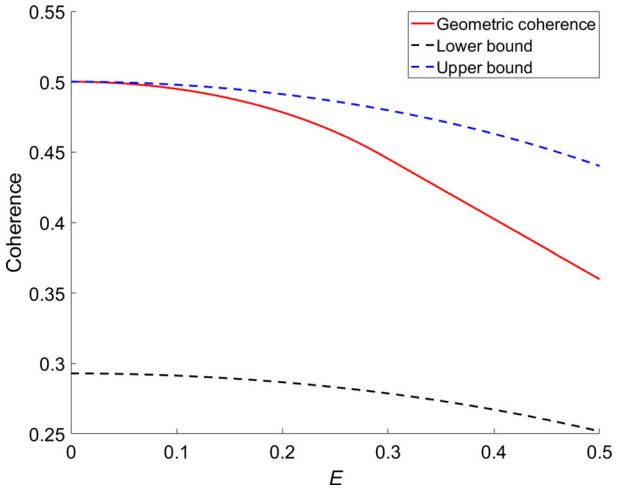

Fig. 3 The variation of geometric coherence and its upper and lower bounds at different E

$\frac{n-nE}{4n} + \frac{nE}{2n}, \frac{n-nE}{4n}\} = \{(1+E)/4, (1-E)/4, (1+E)/4, (1-E)/4\}$. The distribution of '0' and '1' turns to be $\{(1+E)/2, (1-E)/2\}$.

Charlie was able to discriminate quantum states with probability $1-C$ and guess the true value with probability $1/2$ when he fails to discriminate. The existence of covert communication can be detected according to the difference between measurement results with the uniform distribution. Thus, the relationship between coherence and embedding rate is discussed in the following.

The upper and lower bounds of geometric coherence are 1/2-affinity coherence and affinity coherence, respectively, according to Eqs. (8) and (9). For different embedding rate E, the variation of geometric coherence and its upper and lower bounds are shown in Fig. 3.

It can be concluded from Fig. 3 that geometric coherence and 1/2-affinity coherence decrease with the increasing of embedding rate, which means the probability of measuring and successfully recognizing the quantum state will also increase correspondingly. The geometric coherence changes slightly when the embedding rate is low, but decreases dramatically as the embedding rate increases. The difference between 1/2-affinity coherence and geometric coherence is small, while the difference between affinity coherence and geometric coherence is vast. Therefore 1/2-affinity coherence is a substitute for geometric coherence when it is challenging to calculate geometric coherence.

It can be found from Table 1 that, if the embedding rate E is less than 0.1, the change of geometric coherence and 1/2-affinity coherence will be no more than $4e-3$. In this case, quantum states are hard to discriminated and the covert communication is very complicated to be detected for the monitor Charlie. Besides, with the increase of embedding rate, the change of these two kinds of coherence will be significant enough for quantum state discrimination, which is crucial to quantum steganalysis.

Table 1 The values of two coherences at different E values

E	0.05	0.1	0.2	0.3	0.4
C_g	0.4987	0.4949	0.4783	0.4452	0.4024
$C_a^{1/2}$	0.4995	0.4978	0.4911	0.4798	0.4630

The coherence of the quantum channel without covert communication is 0.5, i.e., $C_0 = 0.5$. The theoretical case of distribution $q(x)$ is a uniform distribution. Let us assume that Charlie selects appropriate measurement operators to measure the states with a certain probability, and the detected distribution is $p(x)$. Charlie can judge the existence of covert communication according to the difference between measurement result with the uniform distribution. According to the previous discussion, a steganalysis threshold ξ ought to be set during quantum steganalysis. If $KL(p(x)||q(x)) \geq \xi$, Charlie believes that the channel does exist covert communication and suppresses the transmission. Otherwise, he can resend the measured particles to Bob directly.

5 Performance analysis

5.1 Two essential indicators of quantum steganalysis

Steganographic detection rate and false alarm rate are introduced as two significant performance evaluation indexes of steganalysis. The definitions of steganographic detection rate and false alarm rate are denoted as follows.

Steganographic detection rate (SDR) is the probability of a hidden channel being correctly warned, and it can be denoted by Eq. (24).

$$\mathrm{SDR} = P\left(\mathrm{KL}\left(p'(x)||q(x)\right) \geq \xi\right) \tag{24}$$

False alarm rate (FAR) is the probability that a public quantum channel without hidden channel is incorrectly alarmed, and it can be denoted by Eq. (25).

$$\mathrm{FAR} = P\left(\mathrm{KL}\left(q'(x)||q(x)\right) \geq \xi\right) \tag{25}$$

Here, $q(x)$ is the theoretical distribution, and $p'(x)$ represents the detected distribution of covert communication. Charlie's measurements $q'(x)$ may differ significantly from the theoretical distribution, although there exists no covert communication in the quantum channel.

SDR and FAR can be used to evaluate the performance of quantum steganalysis protocol. In general, for an ideal quantum steganalysis protocol, it should have a high SDR and low FAR. Nevertheless, SDR and FAR are contradictory, which means it is hard for quantum steganalysis protocols to achieve high SDR and low FAR at the same time. If ξ is enlarged, both SDR and FAR will be reduced. Therefore, a suitable value ξ ought to be selected to make a balance.

For the BB84-based quantum steganography protocol whose carriers are pure states, suppose there exist M rounds of QKD transmission between Alice and Bob, and the

monitor Charlie measures N qubits in all. Charlie can discriminate the transmitted states with probability $1 - C$ and guess the true value with probability $1/2$ when he fails to discriminate. So that the distribution of '0' and '1' detected by Charlie is $\left\{\frac{1}{2} + \frac{1}{2}E\left(1 - C\right), \frac{1}{2} - \frac{1}{2}E\left(1 - C\right)\right\}$ in theory. Here, C represents the geometric coherence or 1/2-affinity coherence of ρ^{Q}, which depends on which kind of measurement is used.

The calculation of SDR and FAR of the quantum steganography proposed by Martin has the equivalent forms as:

$$\begin{aligned} \mathrm{SDR} &= 1 - P\left(C_0 - \xi' < \frac{x}{N} < C_0 + \xi'\right) \\ &= 1 - \sum_{C_0 - \xi' < \frac{x}{N} < C_0 + \xi'} \binom{N}{x} a^x \left(1 - a\right)^{N - x} \end{aligned} \tag{26}$$

and

$$\begin{aligned} \mathrm{FAR} &= 1 - P\left(C_0 - \xi' < \frac{y}{N} < C_0 + \xi'\right) \\ &= 1 - \sum_{C_0 - \xi' < \frac{y}{N} < C_0 + \xi'} \binom{N}{y} {C_0}^y \left(1 - C_0\right)^{N - y} \end{aligned} \tag{27}$$

Here, $a = \frac{1}{2} + \frac{1}{2}E\left(1 - C\right)$, C_0 is the coherence of the ρ^{Q} corresponding to the public quantum channel without covert communication, and $\binom{N}{i} = \frac{N!}{i!(N-i)!}$. It can be drawn from the previous calculation that $C_0 = C_g\left(\rho^{Q}\right) = C_a^{1/2}\left(\rho^{Q}\right) = 0.5$.

SDR and FAR are determined by the initial value and variation of coherence and influenced by the detection number N and the threshold ξ. Coherence and embedding rate are negatively correlated. Therefore, the embedding rate is also a fundamental parameter that affects SDR and FAR.

If N or E is enlarged, SDR will increase, while FAR will decrease. If Charlie increases the value of ξ, both SDR and FAR will be lessened. When Charlie suspects that illegal covert communication is underway between Alice and Bob, he could artificially alter the value of threshold ξ to meet different safety requirements. For example, let the embedding rate is 0.2 and N is 300, if $\xi = 0.3 \times 10^{-2}$, then SDR is 0.7653 and FAR is 0.2995; if $\xi = 0.4 \times 10^{-2}$, then SDR is 0.6869 and FAR is 0.2047; if $\xi = 0.5 \times 10^{-2}$, then SDR and FAR would be reduced to 0.6443 and 0.1665, respectively.

In the remainder of this section, the SDR and FAR of the quantum steganography protocol proposed by Martin are calculated, and the parameter ξ is determined by the optimization algorithm with the goal of

$$\min_{\xi} -\mathbf{SDR} + \mathbf{FAR}$$

Charlie can adjust this optimization function if he stresses more about SDR (or FAR).

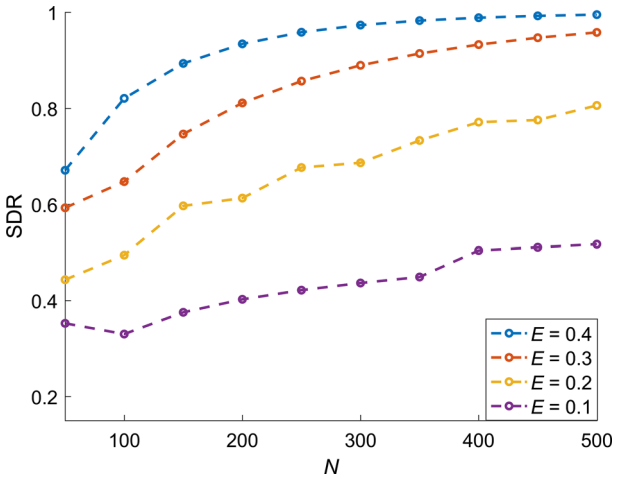

Fig. 4 The variation of geometric coherence-based SDR at different N

The variation of SDR concerning N under different embedding rate E is shown in Fig. 4. Some fluctuations in the curve are due to insufficient detection number N and the optimization algorithm, but we can see the trend that SDR rises with the increase of N and E.

In the optimal threshold ξ, some FAR and SDR values based on two kinds of coherence are figured out and shown in Table 2.

The optimal threshold ξ increases with the increase of E and decreases with the increase of N. In the same detection number, SDR is positively associated with the embedding rate, and FAR is negatively correlated with E. Besides, when the embedding rate is constant, the higher N is, the higher SDR and lower FAR will be achieved. Charlie can improve the performance of the quantum steganalysis protocol by increasing the value of N.

It is worth noting that SDR will be very low, no matter how many numbers that Charlie detects if the embedding rate is minimal. In this case, it is difficult to detect the existence of covert communication. Except for this particular case, the proposed protocol can detect covert communication efficiently and accurately, as long as the embedding rate reaches a certain level.

The results shown in Table 2 can also verify the conclusion that quantum steganalysis has better performance with geometric coherence. For simple cases, we can calculate geometric coherence, while we have to use the sub-optimal choice of 1/2-affinity coherence for some complex cases. Besides, if Charlie does not choose the optimal measurement, the SDR will be slightly reduced.

According to the above analysis, when the steganalysis protocol reaches a specific embedding rate, it has a higher SDR and a lower FAR after certain number of detection. In summary, the performance evaluation result indicates that the proposed quantum steganalysis protocol has a satisfactory performance.

Table 2 FAR and SDR values under optimal ξ

E	N	Geometric coherence			1/2-affinity coherence		
		SDR	FAR	$\xi\left(\times 10^{-2}\right)$	SDR	FAR	$\xi\left(\times 10^{-2}\right)$
0.1	200	0.4027	0.2888	0.39	0.4015	0.2888	0.39
	300	0.4336	0.2726	0.29	0.4350	0.2726	0.31
	400	0.5041	0.2937	0.18	0.5020	0.2937	0.18
	500	0.5171	0.2635	0.17	0.5147	0.2635	0.18
0.2	200	0.6129	0.2292	0.49	0.5991	0.2292	0.56
	300	0.6865	0.1841	0.43	0.7118	0.2253	0.38
	400	0.7712	0.1769	0.34	0.7552	0.1769	0.30
	500	0.8059	0.1399	0.30	0.7896	0.1399	0.30
0.3	200	0.8112	0.1374	0.75	0.7684	0.1374	0.77
	300	0.8896	0.0949	0.65	0.8766	0.1189	0.59
	400	0.9328	0.0642	0.64	0.9172	0.0800	0.56
	500	0.9581	0.0441	0.56	0.9434	0.0544	0.53
0.4	200	0.9342	0.0560	1.31	0.9028	0.0768	1.09
	300	0.9734	0.0242	1.18	0.9585	0.0431	1.02
	400	0.9887	0.0107	1.17	0.9763	0.0187	0.97
	500	0.9951	0.0048	1.11	0.9892	0.0107	0.91

5.2 The steganalysis influence on the normal QKD efficiency

In the process of quantum steganalysis, it is difficult to avoid interference with the normal QKD efficiency, constrained by quantum uncertainty theorem and quantum non-clonability theorem. However, monitor Charlie not only aims to achieve a good steganalysis performance, but also hopes to reduce the interference. Hence, the steganalysis influence on the normal QKD efficiency and the selection of detection rate k are discussed in this section.

Charlie measures N qubits during the quantum steganalysis process in all. Suppose Charlie does a random detection with probability k, i.e., $k = \frac{N}{nM}$. Based on the previous discussion, Charlie was able to discriminate quantum states with success rate $1 - C$, and guess the true value with probability $1/2$ when he fails to discriminate. Here, C represents the geometric coherence or 1/2-affinity coherence of ρ^{Q}. Therefore, this quantum steganalysis process will result in a percentage of errors equal to $kC/2$.

When Charlie suspects that a covert communication is taking place in public quantum channel, he can increase the detection rate k. A large k helps Charlie to confirm the existence of secret messages more quickly with the cost of sacrificing efficiency. In order to reduce the influence of quantum steganalysis on QKD efficiency, Charlie ought to choose a value of k that satisfies

$$\frac{kC}{2} + \frac{3\sqrt{2n\left(\frac{kC}{2}\right)\left(1-\frac{kC}{2}\right)}}{2n} < t$$

$$0 < k < \frac{4nt + 9 - 3\sqrt{-8nt^2 + 8nt + 9}}{(2n + 9)\, C} \tag{28}$$

So that the probability of causing an error rate over the maximum error t allowed by Alice and Bob is minuscule ($t \leq 1/4$), and the detection procedure by Charlie has little impact on the QKD efficiency. This inequality utilizes the normal approximation to a binomial distribution.

Suppose $t = 0.25$ and $C = 0.5$, when $n = 100$, the value of k should be no more than 0.68; when $n = 200$, k should be less than 0.76. Suppose $t = 0.20$ and $C = 0.5$, when $n = 100$, k should be less than 0.51; when $n = 200$, the maximum value of k is 0.585. Charlie can also dynamically select the detection rate k. When k is large occasionally, which would introduce a high error rate over t, Alice and Bob will simply abort the protocol.

In addition, sampling detection is simpler strategy which can also reduce the interference on QKD efficiency. Under this strategy, only a few transmissions will be affected. Charlie can detect all states in one QKD transmission to achieve sufficient detection number, so as to realize effective detection on covert communication. This operation will result in an error exceeding the threshold t, which may be ascribed by Alice and Bob to excessive noise or the presence of some kind of eavesdropping. Alice and Bob can abort this transmission and start another run of QKD.

To sum up, the proposed quantum steganalysis protocol does interfere with the normal QKD efficiency to some extent. Nevertheless, by adjusting the detection rate k or adopting sampling detection strategy, it can effectively reduce the impact on QKD efficiency.

6 Discussions and conclusions

A novel quantum steganalysis protocol targeting pure states is proposed in this paper, which integrates the crucial fact that classical steganography is prone to change the probability distribution of the carrier, and the physical properties that the unknown quantum state discrimination process is sensitive to the distribution. The geometric coherence and affinity coherence are accurately calculated to quantify the probability that the transmitted quantum states can be correctly discriminated. Then effective detection on covert communication can be realized by analyzing the distribution differences after the discrimination. The quantum steganography protocol given by Martin is detailly analyzed in this paper. It is found that, except for the case that the embedding rate is very limited, the performance of the proposed quantum steganalysis protocol will improve dramatically with the increase of embedding rate. Besides, by adjusting the detection rate or adopting sampling detection strategy, the impact on QKD efficiency can be reduced.

The proposed coherence-based quantum steganalysis protocol can not only prevent illegal covert communication, but also serve as a standard for evaluating quantum steganography. The results shown in Tables 1 and 2 can also provide a reference for the design and application of quantum steganography protocol proposed by Martin,

and the selection of different embedding rate can meet diverse levels of imperceptibility requirements.

Acknowledgements This work was supported by the National Natural Science Foundation of China (Nos. 61373131, 61601358, 61303039, 61232016, 61501247), Sichuan Youth Science and Technique Foundation (No. 2017JQ0048), NUIST Research Foundation for Talented Scholars (2015r014), PAPD and CICAEET funds.

References

1. Terhal, B.M., DiVincenzo, D.P., Leung, D.W.: Hiding bits in bell states. Phys. Rev. Lett. **86**(25), 5807 (2001)
2. Guo, G.C., Guo, G.P.: Quantum data hiding with spontaneous parameter down-conversion. Phys. Rev. A **68**(4), 044303 (2003)
3. Eggeling, T., Werner, R.F.: Hiding classical data in multipartite quantum states. Phys. Rev. Lett. **89**(9), 097905 (2002)
4. Matthews, W., Wehner, S., Winter, A.: Distinguishability of quantum states under restricted families of measurements with an application to quantum data hiding. Commun. Math. Phys. **291**(3), 813–843 (2009)
5. El Allati, A., Medeni, M.O., Hassouni, Y.: Quantum steganography via Greenberger–Horne–Zeilinger GHZ4 state. Commun. Theor. Phys. **57**(4), 577–582 (2012)
6. Wang, R.J., Li, D.F., Qin, Z.G.: An immune quantum communication model for dephasing noise using four-qubit cluster state. Int. J. Theor. Phys. **55**(1), 609–616 (2016)
7. Qu, Z.G., Zhu, T.C., Wang, J.W., Wang, X.J.: A novel quantum stegonagraphy based on brown states. CMC: Comput. Mater. Contin. **56**(1), 47–59 (2018)
8. Qu, Z.G., Jiang, L.M., Sun, L., Wang, M.M., Wang, X.J.: Continuous variable quantum steganography protocol based on quantum identity. Math. Biosci. Eng. **16**(5), 4182–4195 (2019)
9. Qu, Z.G., Wu, S.Y., Liu, W.J., Wang, X.J.: Analysis and improvement of steganography protocol based on bell states in noise environment. CMC: Comput. Mater. Contin. **59**(2), 607–624 (2019)
10. Gea-Banacloche, J.: Hiding messages in quantum data. J. Math. Phys. **43**(9), 4531–4536 (2002)
11. Martin, K.: Steganographic Communication with Quantum Information. In: Proceeding of the 9th International Conference on Information Hiding, LNCS 4567, pp. 32–49 (2007)
12. Bennett, C.H., Brassard, G.: Quantum cryptography: public key distribution and coin tossing. In: Proceedings of IEEE International Conference on Computers Systems and Signal Processing, vol. 175, pp. 175–179 (1984)
13. Liao, X., Wen, Q.Y., Sun, Y., Zhang, J.: Multi-party covert communication with steganography and quantum secret sharing. J. Syst. Softw. **83**(10), 1801–1804 (2010)
14. Qu, Z.G., Chen, X.B., Zhou, X.J., Niu, X.X., Yang, Y.X.: Novel quantum steganography with large payload. Opt. Commun. **283**(23), 4782–4786 (2010)
15. Qu, Z.G., Chen, X.B., Luo, M.X., Niu, X.X., Yang, Y.X.: Quantum steganography with large payload based on entanglement swapping of ϕ-type entangled states. Opt. Commun. **284**(7), 2075–2082 (2011)
16. Xu, S.J., Cheng, X.B., Niu, X.X., Yang, Y.X.: A Novel quantum covert channel protocol based on any quantum secure direct communication scheme. Commun. Theor. Phys. **59**(5), 31–37 (2013)
17. Mihara, T.: Quantum steganography using prior entanglement. Phys. Lett. A **379**(12–13), 952–955 (2015)
18. Mihara, T.: Multi-Party quantum steganography. Int. J. Theor. Phys. **56**(2), 576–583 (2017)
19. Qu, Z.G., Wu, S.Y., Wang, M.M., Sun, L., Wang, X.J.: Effect of quantum noise on deterministic remote state preparation of an arbitrary two-particle state via various quantum entangled channels. Quantum Inf. Process. **16**(306), 1–25 (2017)
20. Chen, K., Yan, F., Iliyasu, A.M., Zhao, J.: Exploring the implementation of steganography protocols on quantum audio signals. Int. J. Theor. Phys. **57**(2), 476–494 (2018)
21. Mogos, G.: Stego quantum algorithm. In: International Symposium on Computer Science and its Applications, pp. 187–190 (2008)
22. Mogos, G.: A quantum way to data hiding. Int. J. Multimed. Ubiquitous Eng. **4**(2), 13–20 (2009)

23. Jiang, N., Wang, L.: A novel strategy for quantum image steganography based on Moiré pattern. Int. J. Theor. Phys. **54**(3), 1021–1032 (2015)
24. Heidari, S., Farzadnia, E.: A novel quantum LSB-based steganography method using the Gray code for colored quantum images. Quantum Inf. Process. **16**(10), 242–270 (2017)
25. Luo, G.F., Zhou, R.G., Mao, Y.L.: Two-level information hiding for quantum images using optimal LSB. Quantum Inf. Process. **18**(10), 297 (2019)
26. Qu, Z.G., Li, Z.Y., Xu, G., Wu, S.Y., Wang, X.J.: Quantum image steganography protocol based on quantum image expansion and Grover search algorithm. IEEE Access. **7**, 50849–50857 (2019)
27. Hu, W.W., Zhou, R.G., Liu, X.A., Luo, J., Luo, G.F.: Quantum image steganography algorithm based on modified exploiting modification direction embedding. Quantum Inf. Process. **19**(5), 1–28 (2019)
28. Qu, Z.G., Wen, C.Z., Wang, X.J.: Matrix coding-based quantum image steganography algorithm. IEEE Access. **7**, 35684–35698 (2019)
29. Luo, G.F., Zhou, R.G., Hu, W.W.: Efficient quantum steganography scheme using inverted pattern approach. Quantum Inf. Process. **18**(7), 222 (2019)
30. Luo, J., Zhou, R.G., Hu, W.W., Luo, G.F.: Detection of steganography in quantum gray scale images. Quantum Inf. Process. **19**(5), 1–17 (2020)
31. Chaharlang, J., Mosleh, M., Heikalabad, S.R.: A novel quantum steganography-Steganalysis system for audio signals. Multimed. Tools Appl. **79**, 17551–17577 (2020)
32. Chaharlang, J., Mosleh, M., Heikalabad, S.R.: A novel quantum audio steganography–steganalysis approach using LSFQ-based embedding and QKNN-based classifier. Circ. Syst. Signal Process. **39**, 3925–3957 (2020)
33. Nielsen, M.A., Chuang, I.L.: Quantum Computation and Quantum Information. Cambridge University Press (2000)
34. Luo, S.L., Zhang, Q.: Informational distance on quantum-state space. Phys. Rev. A **69**(3), 032106 (2004)
35. Baumgratz, T., Cramer, M., Plenio, M.B.: Quantifying coherence. Phys. Rev. Lett. **113**(14), 140401 (2014)
36. Streltsov, A., Singh, U., Dhar, H.S., Bera, M.N., Adesso, G.: Measuring quantum coherence with entanglement. Phys. Rev. Lett. **115**(2), 020403 (2015)
37. Xiong, C.H., Kumar, A., Wu, J.D.: Family of coherence measures and duality between quantum coherence and path distinguishability. Phys. Rev. A **98**(3), 032324 (2018)
38. Zhang, H.J., Chen, B., Li, M., Fei, S.M., Long, G.L.: Estimation on geometric measure of quantum coherence. Commun. Theor. Phys. **67**(2), 166–170 (2017)
39. Belavkin, V.P.: Optimal multiple quantum statistical hypothesis testing. Stoch.: Int. J. Probab. Stoch. Process. **1**(1–4), 315–345 (1975)
40. Holevo, A.S.: On asymptotically optimal hypotheses testing in quantum statistics. Teor. Veroyatnostei Primen. **23**(2), 429–432 (1978)
41. Eldar, Y.C., Forney, G.D.: On quantum detection and the square-root measurement. IEEE Trans. Inf. Theory **47**(3), 858–872 (2001)
42. Spehner, D.: Quantum correlations and distinguishability of quantum states. J. Math. Phys. **55**(7), 075211 (2014)
43. Xiong, C.H., Wu, J.D.: Geometric coherence and quantum state discrimination. J. Phys. A: Math. Theor. **51**(41), 414005 (2018)

Affiliations

Zhiguo Qu[1,2,3] · Yiming Huang[4] · Min Zheng[5]

✉ Zhiguo Qu
qzghhh@126.com

✉ Min Zheng
zmyjl761218@163.com

Yiming Huang
huangyiming1999@yeah.net

1 Jiangsu Collaborative Innovation Center of Atmospheric Environment and Equipment Technology, Nanjing University of Information Science and Technology, Nanjing, China

2 Engineering Research Center of Digital Forensics, Ministry of Education, Nanjing University of Information Science and Technology, Nanjing, China

3 School of Computer and Software, Nanjing University of Information Science and Technology, Nanjing, China

4 Changwang School of Honors, Nanjing University of Information Science and Technology, Nanjing, China

5 Hubei University of Science and Technology, Xianning, China